Available online at www.sciencedirect.com
SCIENCE DIRECT®
Bioorganic & Medicinal Chemistry Letters 15 (2005) 5531–5536
Bioorganic & Medicinal Chemistry Letters

Recognition of a 10 base pair sequence of DNA and stereochemical control of the binding affinity of chiral hairpin polyamide–Hoechst 33258 conjugates

Putta Mallikarjuna Reddy, Joseph W. Toporowski, Alexandra L. Kahane and Thomas C. Bruice*

Department of Chemistry and Biochemistry, University of California at Santa Barbara, Santa Barbara, CA 93106, USA

Received 8 July 2005; revised 24 August 2005; accepted 25 August 2005
Available online 3 October 2005

Abstract—Chiral hairpin polyamides linked to a Hoechst 33258 analogue at the α-position of the hairpin turn amino acid (**1**, **2**) were synthesized on solid phase by adopting Fmoc and ivDde techniques. The DNA-binding properties of enantiomeric conjugates **1** and **2**, and *N*-terminal linked conjugate **3** for 8–14 bp sequences were determined by spectrofluorometric and thermal melting studies. Conjugates **1** and **2** recognize a 10 bp sequence, while conjugate **3** recognizes a 9 bp sequence. Interestingly, *R*-enantiomer **1** exhibited 10- to 30-fold higher binding affinities than *S*-enantiomer **2** for the DNA sequences studied. These binding differences were accounted for by molecular modeling studies, which revealed that the amide proton nearest to the chiral center in *R*-conjugate **1** is better positioned to form hydrogen bonds to the DNA bases, while *S*-conjugate **2** does not.

The development of DNA-binding ligands capable of recognizing longer sequences with high affinity and sequence specificity is essential to control a specific gene's expression, thereby curing the disease rather than simply treating the symptoms. Synthetic polyamides consisting of *N*-methylpyrrole (Py) and *N*-methylimidazole (Im) amino acids have shown binding affinities and sequence specificities comparable to those of natural DNA-binding proteins.[1] Furthermore, head-to-tail linkage of such polyamides with γ-aminobutyric acid (γ) provides hairpin polyamides that mimic the 2:1 side-by-side antiparallel binding of the unlinked polyamides and bind to specifically designed target sites with 100-fold enhanced affinity relative to unlinked polyamides.[1,2] Although these polyamides have the potential to modulate gene expression by blocking the activation of transcription factors,[3] their use as drugs is limited because they can only recognize 5–6 base pairs (bp). To specifically discriminate different genes, it is necessary to target longer DNA sequences. Studies of polyamide binding-site size limitations suggest that beyond five consecutive rings, the ligand's curvature fails to match the pitch of the DNA double helix, disrupting the hydrogen bonds and van der Waals interactions necessary for specific DNA sequence recognition.[4] Furthermore, attempts to inhibit the transcription of endogenous genes in cell lines other than insects or T-lymphocytes have met with little success, presumably due to poor cellular uptake of these polyamides and inability to achieve nuclear localization.[5]

Recent studies have shown that linkage of polyamides to minor groove binding bis-benzimidazole dyes can recognize longer sequences of DNA and also enhance cellular permeability.[6,7] Furthermore, linkage of the Hoechst 33258 fluorophore to the six-ring hairpin pyrrole polyamide at the *N*-terminus (**3**) recognizes a 9 bp A/T-rich site with high affinity and good selectivity.[8] This conjugate binds to the 9 bp site with 1:1 stoichiometry with the polyamide moiety adopting a hairpin motif. However, the binding motif of this conjugate is unknown in the presence of sequences longer than 10 bp. The sequence recognition and discrimination of DNA by polyamides depend on the code of side-by-side amino acid pairings in the minor groove.[1] Recent studies have shown that incorporation of bulky groups on the linker-turn forces the polyamide to adopt a hairpin motif instead of an

Keywords: Chiral hairpin polyamide–Hoechst 33258 conjugates.
* Corresponding author. Tel.: +1 805 893 2044; fax: +1 805 893 2229; e-mail: tcbruice@chem.ucsb.edu

0960-894X/$ - see front matter © 2005 Elsevier Ltd. All rights reserved.
doi:10.1016/j.bmcl.2005.08.076

extended motif.[9] We presume that linkage of the Hoechst ligand at the hairpin turn may force the polyamide to adopt the hairpin motif irrespective of minor groove length and provide side-by-side amino acid pairings, which is a prerequisite for sequence specific recognition. Furthermore, these conjugates might be able to recognize longer DNA sequences, and the presence of the Hoechst fluorophore should enhance cellular uptake.[7] The relationships between the Hoechst linkage position in the polyamide, the binding site size, and the cellular uptake of the conjugates have yet to be determined. To evaluate these considerations, a new class of chiral hairpin polyamide–Hoechst 33258 conjugates was designed.

Following pioneering work by Dervan and co-workers,[10] replacement of the prochiral γ-aminobutyric acid turn with either enantiomer of 2,4-diaminobutyric acid and linkage of the Hoechst 33258 analogue at the α-amino position provides the enantiomeric conjugates Py–Py–Py–γ-[(*R*)-γ-Ht]–Py–Py–Py (**1**) and Py–Py–Py–γ-[(*S*)-γ-Ht]–Py–Py–Py (**2**) (Fig. 1). Dervan and co-workers found that (*R*)-configured amine γ-turn substituents enhance DNA-binding affinity and specificity relative to the unsubstituted parent hairpin,[10a] and it was of interest to investigate the effects of relocating the position of the Hoechst 33258 analogue. The conjugates were synthesized on solid phase using Fmoc and ivDde techniques with a series of HOBt/PyBOP mediated coupling reactions. To compare the binding affinity to the binding site length, the conjugate Py–Py–Py–γ-Py–Py–Py–γ-Ht (**3**) with the Hoechst fluorophore linked to the *N*-terminus of the polyamide was also studied (Fig. 1).[8] The fluorescence emission of these conjugates increases greatly upon binding in the minor groove of dsDNA. Thus, spectrofluorometric titrations were employed to determine the conjugate:dsDNA stoichiometries and equilibrium association constants (K_a).[6,8] Thermal melting (T_m) experiments were also performed as an alternative method for the determination of the conjugate:dsDNA complex stabilities. We report here the synthesis, DNA binding affinity, binding site length, and binding orientation of conjugates **1**–**3** to A/T-rich 8–14 bp sequences.

The solid-phase synthesis of conjugates **1** and **2** were accomplished manually in a stepwise manner on rink amide MBHA resin (0.5 mmol/g loading sites) by employing Fmoc and ivDde techniques with a series of PyBOP/HOBt mediated coupling reactions as described in Scheme 1. The linker ivDde-protecting group is best suited for this solid-phase synthesis because it is stable under Fmoc deprotection conditions and can easily be removed using 5% hydrazine in DMF. The Fmoc-Py-OH (**4**)[11] and Hoechst 33258 acid (**7**)[12] building blocks were synthesized as reported, and orthogonally protected 2,4-diaminobutyric acid residues Fmoc-D-Dab(ivDde)-OH (**5**) and Fmoc-Dab(Mtt)-OH (**6**) were purchased from Chem-Impex and Novabiochem, respectively (Fig. 2).

The solid-phase synthesis of the *R*-conjugate, **1**, is shown in (Scheme 1). The Fmoc protection on the resin was removed and the coupling of Fmoc-Py-acid (**4**) was achieved in 12 h in the presence of HOBt, PyBOP, and DIPEA in anhydrous DMF. After the coupling reaction, any unreacted amine sites were capped by acetylation. The Fmoc protection on the *N*-methylpyrrole was removed and the coupling cycle (coupling/capping/deprotection) was repeated two more times with Fmoc-Py-OH (**4**) before introducing orthogonally protected 2,4-diaminobutyric acid (Fmoc-D-Dab(ivDde)-OH) (**5**). The Fmoc protection of the linker α-amino group was removed and coupled with Hoechst 33258 acid (**7**). After the capping reaction, the ivDde protection on the γ-amino group was removed using 5% hydrazine in DMF and the coupling cycle was repeated three more times with Fmoc-Py-OH (**4**). The Fmoc on

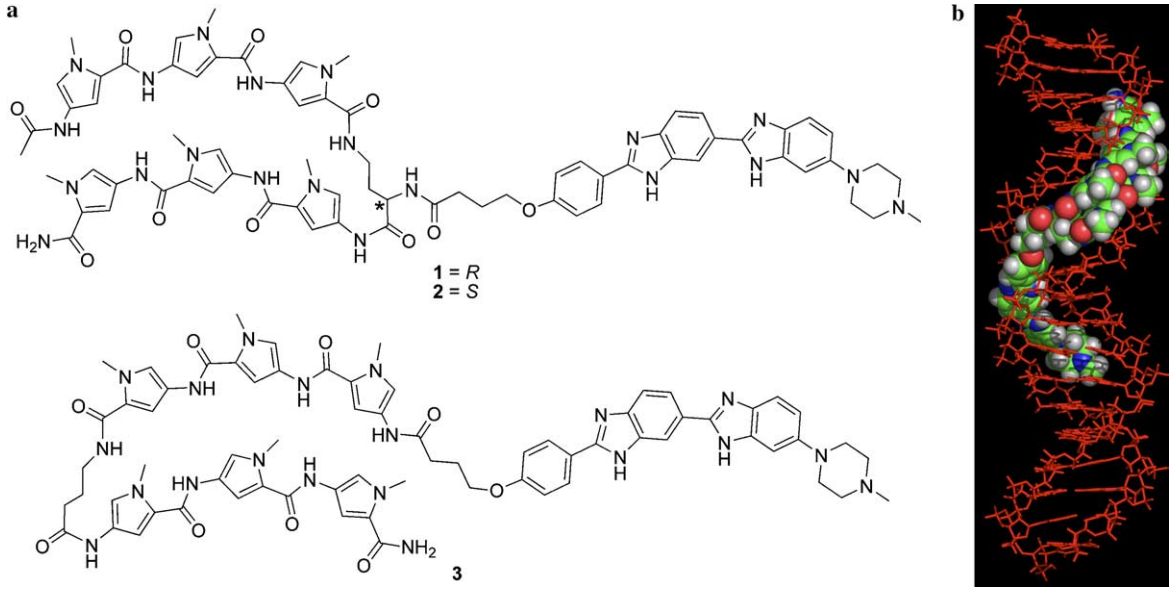

Figure 1. (a) Structures of the hairpin pyrrole polyamide–Hoechst 33258 conjugates (**1**–**3**). (b) Energy minimized complex of **1** bound to the minor groove of d(5′-GCGGATATAAAATTC-GACG-3′).

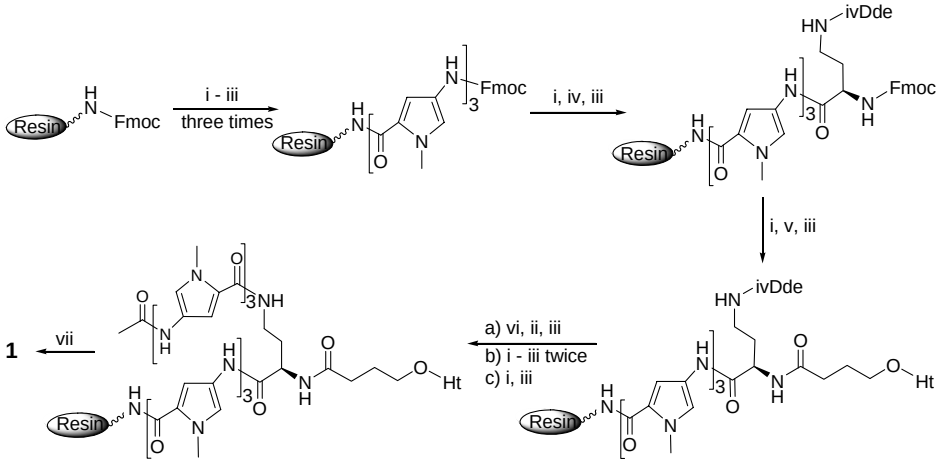

Scheme 1. Reagents and conditions: (i) Deprotection: 20% piperidine/DMF, 15 min; (ii) coupling: Fmoc-Py-OH (**4**), PyBOP, HOBt, DIPEA, DMF, 12 h; (iii) capping: acetic anhydride, TEA, DMF, 10 min; (iv) coupling: Fmoc-D-Dab(ivDde)-OH (**5**), PyBOP, HOBt, DIPEA, DMF, 12 h; (v) coupling: Hoechst 33258 acid (**7**), PyBOP, HOBt, DIPEA, DMF, 24 h; (vi) deprotection: 5% hydrazine in DMF (2 × 5 min); (vii) cleavage: TFA, TIS, 2 h. Ht = Hoechst 33258.

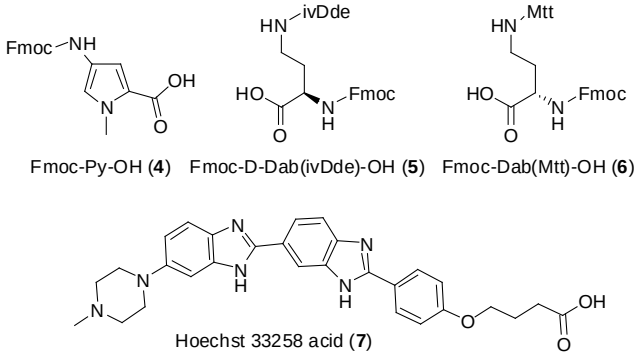

Figure 2. Monomers for the solid phase synthesis of conjugates **1**–**2**.

the last pyrrole was removed and the amine was capped to get conjugate **1**. The coupling yield in each cycle was found to be 95–99%, as determined from the absorbance of deprotected Fmoc. The conjugate was cleaved from the resin in 2 h using 1% triisopropylsilane (TIS) in TFA. The cleaved products were purified on reverse-phase HPLC using a C_8 column with an increasing gradient of acetonitrile in water containing 0.1% TFA. After purification, the product was reconstituted in a minimal amount of methanol and precipitated out of solution by the addition of ether. Product purity was checked by analytical RP-HPLC using the same column and solvent system. ESI/TOF+ mass analysis exhibited the expected peak at *m*/*z* 692.79 (M+2H) for conjugate **1**; calcd 692.81 (M+2H) for $C_{71}H_{77}N_{21}O_{10}$.

Conjugate **2** was also synthesized in a similar method, as explained above for conjugate **1**, using Fmoc-Dab(Mtt)-OH (**6**) instead of Fmoc-D-Dab(ivDde)-OH **5**. The acid labile Mtt protection on the γ-amino group was removed using 1% TFA and 5% TIS in dichloromethane (5 × 5 min).[13] However, under these conditions the TFA solution cleaved some of the conjugate from the resin along with the cleavage of Mtt on the γ-amino group of the linker. Hence, the base labile ivDde protection of the γ-amino group of the linker is better suited for the solid-phase synthesis of these conjugates. The resin cleavage and purification of the conjugate **2** was carried out as explained for conjugate **1**. ESI/TOF+ mass analysis exhibited the expected peak at *m*/*z* 692.82 (M+2H) for conjugate **2**; calcd 692.81 (M+2H) for $C_{71}H_{77}N_{21}O_{10}$.

When excited at 345 nm, dsDNA:conjugate complexes in 10 mM potassium phosphate buffer (pH 7.0) containing 150 mM KCl solution emit a broad fluorescence signal centered at 450 nm (**1** and **3**) or 455 nm (**2**), which is consistent with the fluorescence signal emitted by Ht33258:dsDNA complexes at 445 nm.[14,15] Titration of a constant concentration of dsDNA with a relatively concentrated solution of conjugate **1**, **2**, or **3** provided a well-defined titration curve that allowed the determination of the conjugate:dsDNA complex stoichiometry.[6,16] The equilibrium association constants (K_a) for the dsDNA:conjugate complexes were determined by generating isothermal binding curves (fluorescence vs unbound conjugate) and fitting the equation as shown in Figure 3.[6,8,17]

In order to understand the binding affinities, binding site length, and binding orientation of conjugates **1**–**3**, a series of dsDNA with A/T-rich 8–14 bp binding sites (Table 1) were used. Conjugates **1**–**3** exhibited ~1:1 dsDNA:conjugate stoichiometries with each of the DNA duplexes. With longer binding sites, side-by-side 1:2 antiparallel binding is feasible[6a] with conjugate **3** if the polyamide prefers the extended motif upon binding. Very little change in stoichiometry was observed in the binding of conjugate **3** to a 14 bp sequence (entry 7), which is an adequate length to allow for binding in the extended form and side-by-side antiparallel binding. This suggests that the polyamide moiety of conjugate **3** prefers a hairpin orientation,[8] rather than an extended or dimeric overlapped binding motif. As can be seen from the K_a data in Table 1, conjugate **3** recognizes the 9 bp A/T-rich binding site of 5′-gcggTATAAA ATTcgacg-3′ (entry 2) with high affinity.[8] Very little

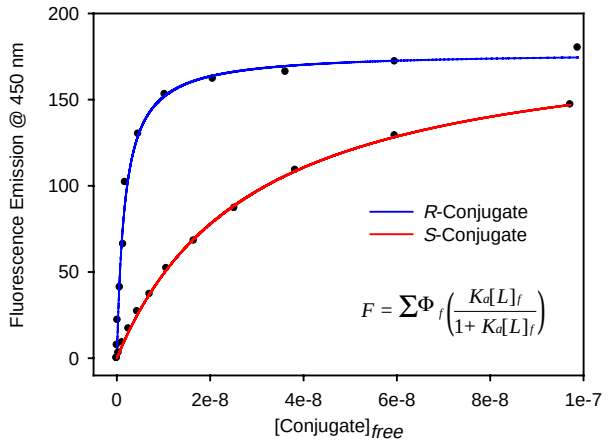

Figure 3. Titration of a 10 nM dsDNA (entry 4) in 10 mM potassium phosphate buffer (pH 7) containing 150 mM KCl solution with 1 μM of conjugates **1** and **2** in DMSO. Isothermal binding curves generated from fluorescence intensity versus concentration of unbound conjugates **1** or **2**, and then data points were fitted using the equation[17] shown in the figure.

change in K_a and binding stoichiometry was observed upon extending the A/T-rich binding site from 9 to 14 bp (entries 2–7). However, a considerable drop in K_a was observed upon decreasing the binding site length to 8 bp (entry 1), indicating that the conjugate binds to a 9 bp sequence. On the other hand, conjugates **1** and **2** bind to the 10 bp A/T-rich site of 5′-gcggATATAAA ATTcgacg-3′ (entry 3). Although a moderate increase in K_a was exhibited upon increasing the binding site from 10 to 14 bp (entries 4–7), considerable drops in K_a were observed in the presence of binding sites shorter than 10 bp (entries 1–2). These observations suggest that conjugates **1** and **2** can recognize 10 bp sequences, whereas conjugate **3** can recognize only 9 bp.[8] Interestingly, conjugates **1** and **3** exhibited similar binding affinities for their preferred 10 and 9 bp sequences, respectively, suggesting that the linkage position does not significantly affect binding affinity. However, the dsDNA sequences exhibited remarkable preference for the chiral conjugate **1** over **2**. Although both conjugates **1** and **2** can bind to 10 bp sequences (Table 1), the *R*-conjugate **1** consistently exhibited higher (~10- to 20-fold) binding affinities than the *S*-conjugate **2** for the sequences studied.

Thermal denaturation experiments were employed as an alternative method for the investigation of the dsDNA:conjugate complex stabilities and sequence selectivities. As shown in Table 1, the T_m data strongly correlate with the data acquired via the equilibrium assays. Conjugates **1** and **3** form significantly more stable complexes than does conjugate **2**. Conjugate **1** forms a stable complex with the 10 bp (ΔT_m = 22 °C) sequence (entry 3). The stability of the complex suffered greatly when providing a binding site shorter than 10 bp (entries 1 and 2); however, no significant change in ΔT_m was observed upon the extension of the binding site from 10 to 14 bp. Although *S*-conjugate **2** forms less stable complexes, it displays binding patterns similar to those of the *R*-conjugate **1**. Conjugate **3** also forms stable complexes, however, it recognizes only 9 bp (entry 2). When provided a 14 bp sequence, a length sufficient to bind the extended or 1:2 side-by-side overlapped motif, a moderate change in ΔT_m is observed for conjugate **3**, which also suggests that the polyamide moiety prefers a hairpin motif. To describe the complex stabilities more quantitatively, standard free energies (ΔG^0_{25}) for both *R*- and *S*-conjugate:dsDNA complexes were calculated from thermal melting curves (Table 1). The $\Delta\Delta G^0$ values of −1.2 to −2.4 kcal/mol suggest that *R*-conjugate **1** has about ~10- to 50-fold higher binding affinity than the *S*-conjugate **2** to the dsDNA sequences, which is consistent with the observed binding constants (Table 1).

To further explore the observed differences in the binding affinities of enantiomers **1** and **2**, molecular modeling was performed using Sybyl.[18] Canonical B-DNA duplex d(5′-GCGGAT-ATAAAATTCGACG-3′) was built using the biopolymer function. Conjugates **1** and **2** were assembled by extracting two distamycin molecules which were bound side-by-side in the minor groove of a DNA duplex from the PDB structure 378D,[19] and connecting them with an appropriate linker. A Hoechst 33258 ligand was extracted from a DNA crystal structure from PDB entry 264D,[20] and attached to the polyamide hairpin linker, being careful to create the proper stereochemistry. Hydrogens were then added to the DNA and ligand models, the atom types were properly assigned, and Pullman charges were calculated. Since the models of **1** and **2** were assembled from crystal structures, they were already in the approximate orientation to bind into the minor groove of the DNA model. This

Table 1. Thermal melting temperatures (T_m in °C) and equilibrium association constants (K_a) for conjugate:dsDNA complexes

Entry	dsDNA	ΔT_m			$\Delta\Delta G$ (kcal)	K_a		
		1(*R*)	**2**(*S*)	**3**		**1**(*R*)	**2**(*S*)	**3**
1	5′-gcggcATAAAATTcgacg-3′	15	7	14	−0.8	2.3×10^8	5.3×10^7	4.1×10^8
2	5′-gcggTATAAAATTcgacg-3′	14	6	24	−1.4	1.7×10^8	3.4×10^7	2.2×10^9
3	5′-gcggATATAAAATTcgacg-3′	22	11	23	−2.1	2.4×10^9	1.6×10^8	3.3×10^9
4	5′-gcggAATATAAAATTcgacg-3′	23	11	23	−2.3	2.7×10^9	3.1×10^8	2.7×10^9
5	5′-gcggTAATATAAAATTcgacg-3′	21	10	22	−2.4	1.2×10^9	1.0×10^8	3.1×10^9
6	5′-gcggATAATATAAAATTcgacg-3′	22	11	24	–2.4	2.2×10^9	8.5×10^7	2.5×10^9
7	5′-gcggTATAATATAAAATTcgacg-3′	22	10	24	−2.4	1.8×10^9	9.8×10^7	4.2×10^9

Binding sites shown in capitals. Standard deviations are ± 1 °C and ± 20% for T_m and K_a, respectively. ΔT_m values are the differences in the T_m values of dsDNA in the presence and absence of the conjugate. ΔG_{25} values are calculated from T_m curves. $\Delta\Delta G$ values are the differences between the *R*- and *S*-conjugate ΔG_{25} values.

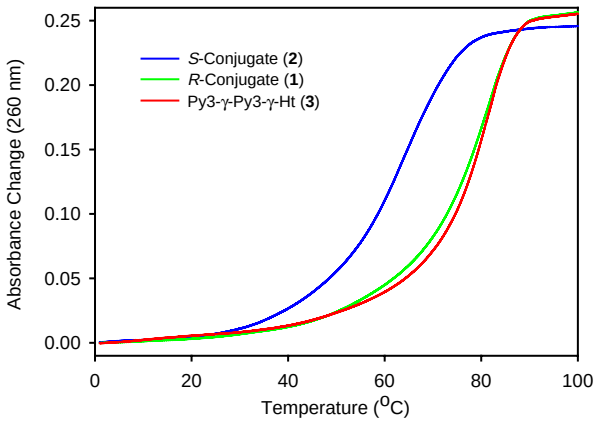

Figure 4. Normalized T_m curves for dsDNA (2 μM) in the presence of 2 equiv of conjugate **1** (with dsDNA entry 3), conjugate **2** (with dsDNA entry 3), and conjugate **3** (with dsDNA entry 2) in 10 mM potassium phosphate buffer (pH 7) containing 150 mM KCl.

allowed the ligands to be carefully hand-placed into the minor groove, before the energy was minimized using the Tripos forcefield. The ligands were then docked into the minor groove, and a quick energy minimization was performed. The molecular graphics were created using PyMOL[21] (Fig. 4).

The molecular modeling studies involving energy minimizations revealed that the different geometries of enantiomers **1** and **2** lead to differences in hydrogen bonding patterns upon DNA minor groove binding. The amide proton at the α-position of the chiral center in *R*-conjugate **1** is in an ideal position to form a hydrogen bond with the O_2 of thymine 13 (Fig. 5a). This amide proton in *S*-conjugate **2**, however, is oriented away from the O2 atom and lies far enough away to prohibit hydrogen bond formation (Fig. 5b). In addition to the location and orientation of the amide proton α to the chiral center, the two amide protons further down the polyamide chains are also better positioned for hydrogen bonds to the DNA bases in the *R*-configured **1** versus *S*-configured **2** (Figs. 5a and b). Although the amide proton, shown with a dashed line to N3 of adenine 14, is too far away for a proper hydrogen bond in either enantiomers, it lies closer to N3 in **1** (Fig. 5a) than in **2** (Fig. 5b). The remaining nitrogen-bound protons on the polyamide and Hoechst chains demonstrate similar patterns for both enantiomers, generally forming solid hydrogen bonds with the DNA bases. Altogether, the modeling study suggests that the greater binding affinities observed when **1** binds in the DNA minor groove versus when **2** binds can be accounted for by the enhanced ability of **1** to form hydrogen bonds to the DNA bases.

Linkage of the Hoechst 33258 analogue at the α-position of the γ-turn amino acid recognizes 10 bp DNA sequences, whereas the *N*-terminus linked conjugate recognizes 9 bp sequences with the polyamide adopting a hairpin motif. Although the linkage position of the Hoechst dye did not significantly affect binding affinity, the dsDNA sequences exhibited considerable preference for the *R*-conjugate over the *S*-conjugate. The synthesis of conjugates incorporating both *N*-methylpyrrole and *N*-methylimidazole units and studies on their cellular uptake are in progress. These mixed heterocyclic conjugates will be able to target sequences containing both A/T and G/C bp.

Acknowledgment

This work was supported by a grant from the National Institute of Health (5R37DK09171-36).

References and notes

1. Dervan, P. B. *Bioorg. Med. Chem.* **2001**, *9*, 2215.
2. (a) Mrksich, M.; Parks, M. E.; Dervan, P. B. *J. Am. Chem. Soc.* **1994**, *116*, 7983; (b) Parks, M. E.; Baird, E. E.; Dervan, P. B. *J. Am. Chem. Soc.* **1996**, *118*, 6147; (c) Parks, M. E.; Baird, E. E.; Dervan, P. B. *J. Am. Chem. Soc.* **1996**, *118*, 6153; (d) Trauger, J. W.; Baird, E. E.;

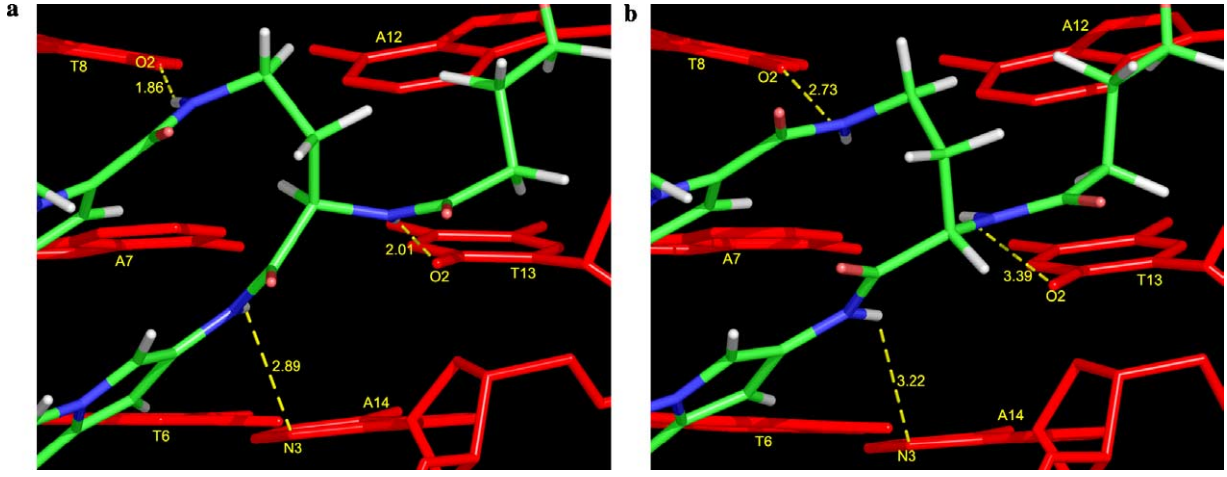

Figure 5. Closeup of the hairpin linker of (a) *R*-enantiomer **1** and (b) *S*-enantiomer **2** bound in the minor groove of d(5′-GCGGATATAAA-ATTCGACG-3′). The dashed lines show the amide protons' nearest potential hydrogen bond acceptor, with the proton–proton acceptor distances, acceptor names, and nucleotide names labeled.

Dervan, P. B. *Chem. Biol.* **1996**, *3*, 369; (e) Swalley, S. E.; Baird, E. E.; Dervan, P. B. *J. Am. Chem. Soc.* **1996**, *118*, 8198; (f) Pilch, D. S.; Pokar, N. A.; Gelfand, C. A.; Law, S. M.; Breslauer, K. J.; Baird, E. E.; Dervan, P. B. *Proc. Natl. Acad Sci. U.S.A.* **1996**, *93*, 8306; (g) de Claire, R. P. L.; Geierstanger, B. H.; Mrksich, M.; Dervan, P. B.; Wemmer, D. E. *J. Am. Chem. Soc.* **1997**, *119*, 7909.

3. (a) Gottesfeld, J. M.; Neeley, L.; Trauger, J. W.; Baird, E. E.; Dervan, P. B. *Nature* **1997**, *387*, 202; (b) Mapp, A. M.; Ansari, A. Z.; Ptashne, M.; Dervan, P. B. *Proc. Natl. Acad Sci. U.S.A.* **2000**, *97*, 3930.
4. (a) Kelly, J. J.; Baird, E. E.; Dervan, P. B. *Proc. Natl. Acad. Sci. U.S.A.* **1996**, *93*, 6981; (b) Kielkopf, C. L.; Baird, E. E.; Dervan, P. B.; Rees, D. C. *Nat. Struct. Biol.* **1998**, *5*, 104.
5. Chiang, S. Y.; Burli, R. W.; Benz, C. C.; Gawron, L.; Scott, G. K.; Dervan, P. B.; Beerman, T. A. *J. Biol. Chem.* **2000**, *275*, 24246.
6. (a) Satz, A. L.; Bruice, T. C. *J. Am. Chem. Soc.* **2001**, *123*, 2469; (b) Satz, A. L.; Bruice, T. C. *Bioorg. Med. Chem.* **2002**, *10*, 241; (c) Reddy, P. M.; Jindra, P. T.; Satz, A. L.; Bruice, T. C. *J. Am. Chem. Soc.* **2003**, *125*, 7843.
7. (a) White, C. M.; Satz, A. L.; Bruice, T. C.; Beerman, T. A. *Proc. Natl. Acad. Sci. U.S.A.* **2001**, *98*, 10590; (b) White, C. M.; Satz, A. L.; Gawron, L. S.; Bruice, T. C.; Beerman, T. A. *Biochim. Biophys. Acta* **2001**, *1574*, 100.
8. Reddy, P. M.; Dexter, R.; Bruice, T. C. *Bioorg. Med. Chem. Lett.* **2004**, *14*, 3803.
9. Woods, C. R.; Ishii, T.; Wu, B.; Bair, K. W.; Boger, D. L. *J. Am. Chem. Soc.* **2002**, *124*, 2148.
10. (a) Herman, D. M.; Baird, E. E.; Dervan, P. B. *J. Am. Chem. Soc.* **1998**, *120*, 1382; (b) Herman, D. M.; Baird, E. E.; Dervan, P. B. *Chem. Eur. J.* **1999**, *5*, 975; (c) Trauger, J. W.; Baird, E. E.; Dervan, P. B. *Chem. Biol.* **1996**, *3*, 369.
11. Wurtz, N. R.; Turner, J. M.; Baird, E. E.; Dervan, P. B. *Org. Lett.* **2001**, *3*, 1201.
12. Reddy, P. M.; Bruice, T. C. *J. Am. Chem. Soc.* **2004**, *126*, 3736.
13. Park, C.; Burgess, K. *J. Comb. Chem.* **2001**, *3*, 257.
14. (a) Chiang, S. –Y.; Bruice, T. C.; Azizkhan, J. C.; Gawron, L.; Beerman, T. *Proc. Natl. Acad. Sci. U.S.A.* **1997**, *94*, 2811; (b) He, G. X.; Browne, K. A.; Blasko, A.; Bruice, T. C. *J. Am. Chem. Soc.* **1994**, *116*, 3716; (c) Browne, K. A.; He, G. X.; Bruice, T. C. *J. Am. Chem. Soc.* **1993**, *115*, 7072.
15. (a) Loontiens, F. G.; Regenfuss, P.; Zechel, A.; Dumortier, L.; Clegg, R. M. *Biochemistry* **1990**, *29*, 9029; (b) Bostock-Smith, C. E.; Searle, M. S. *Nucleic Acids Res.* **1999**, *27*, 1619; (c) Haq, I.; Ladbury, J. E.; Chowdhry, B. Z.; Jenkins, T. C.; Chaires, J. B. *J. Mol. Biol.* **1997**, *271*, 244; (d) Loontiens, F. G.; McLaughlin, L. W.; Diekmann, S.; Clegg, R. M. *Biochemistry* **1991**, *30*, 182.
16. The point of intersection of the two straight lines generated by fitting the pre- and post-saturation data points in the titration over *x*-axis provided the stoichiometry of conjugate:dsDNA complex.
17. (a) Browne, K. A.; He, G. X.; Bruice, T. C. *J. Am. Chem. Soc.* **1993**, *115*, 7072; (b) Satz, A. L.; Bruice, T. C. *Bioorg. Med. Chem.* **2000**, *8*, 1871.
18. Sybyl, version 6.8, 2001 Tripos, St. Louis, MO.
19. Mitra, S. N.; Wahl, M. C.; Sundaralingam, M. *Acta Crystallogr.* **1999**, *D55*, 602.
20. Vega, M. C.; Saez, I. G.; Aymami, J.; Eritja, R.; van deer Marel, G. A.; van Boom, J. H.; Rich, A.; Coll, M. *Eur. J. Biochem.* **1994**, *222*, 721.
21. Delano W. L, 'The PyMOL Graphics System.' version 0.97, 2004, Delano Scientific LLC, San Carlos, CA, USA. http://www.pymol.org.